

Ferroelectric C* phase induced in a nematic liquid crystal matrix by a chiral non-mesogenic dopant

Original

Ferroelectric C* phase induced in a nematic liquid crystal matrix by a chiral non-mesogenic dopant / Pozhidaev, E.P., Torgova, S.I., Barbashov, V.A., Minchenko, M.V., Sulyanov, S.N., Dorovatovskii, P.V., Ostrovskii, B.I., Strigazzi, A.. - In: APPLIED PHYSICS LETTERS. - ISSN 0003-6951. - 106:6(2015), p. 062904. [10.1063/1.4908152]

Availability:

This version is available at: 11583/2616331 since: 2015-09-01T14:35:06Z

Publisher:

AIP Publishing

Published

DOI:10.1063/1.4908152

Terms of use:

This article is made available under terms and conditions as specified in the corresponding bibliographic description in the repository

Publisher copyright

(Article begins on next page)

Ferroelectric C* phase induced in a nematic liquid crystal matrix by a chiral non-mesogenic dopant

E. P. Pozhidaev, S. I. Torgova, V. A. Barbashov, M. V. Minchenko, S. N. Sulyanov, P. V. Dorovatovskii, B. I. Ostrovskii, and A. Strigazzi

Citation: *Applied Physics Letters* **106**, 062904 (2015); doi: 10.1063/1.4908152

View online: <http://dx.doi.org/10.1063/1.4908152>

View Table of Contents: <http://scitation.aip.org/content/aip/journal/apl/106/6?ver=pdfcov>

Published by the [AIP Publishing](#)

Articles you may be interested in

[Wavelength tuning the photonic band gap in chiral nematic liquid crystals using electrically commanded surfaces](#)
Appl. Phys. Lett. **91**, 231110 (2007); 10.1063/1.2820681

[The influence of fluorosurfactants on the flexoelectro-optic properties of a chiral nematic liquid crystal](#)
J. Appl. Phys. **101**, 114109 (2007); 10.1063/1.2743820

[Generation of frustrated liquid crystal phases by mixing an achiral nematic–smectic-C mesogen with an antiferroelectric chiral smectic liquid crystal](#)
J. Chem. Phys. **122**, 144906 (2005); 10.1063/1.1872753


[Photoinduced layer alignment control in ferroelectric liquid crystal with N*–C* phase transition doped with photochromic dye](#)
Appl. Phys. Lett. **76**, 1228 (2000); 10.1063/1.125992

[Calculation of helical twisting power for liquid crystal chiral dopants](#)
J. Chem. Phys. **112**, 1560 (2000); 10.1063/1.480703



AIP | Applied Physics
Letters

Meet The New Deputy Editors

	Alexander A. Balandin		Qing Hu		David L. Price
---	--------------------------	---	---------	--	-------------------

Ferroelectric C* phase induced in a nematic liquid crystal matrix by a chiral non-mesogenic dopant

E. P. Pozhidaev,¹ S. I. Torgova,^{1,4} V. A. Barbashov,¹ M. V. Minchenko,¹ S. N. Sulyanov,² P. V. Dorovatovskii,³ B. I. Ostrovskii,^{2,5} and A. Strigazzi^{4,6,a)}

¹*P. N. Lebedev Physics Institute of the Russian Academy of Sciences, Leninsky pr. 53, Moscow 119991, Russia*

²*Shubnikov Institute of Crystallography of the Russian Academy of Sciences, Leninsky pr. 59, Moscow 119333, Russia*

³*Kurchatov Centre, Kurchatov sq. 1, Moscow 123182, Russia*

⁴*Department of Applied Science and Technology, Physics Institute of Condensed Matter and Complex Systems, CNISM, Politecnico di Torino, corso Duca degli Abruzzi 24, I-10129 Torino, Italy*

⁵*Landau Institute for Theoretical Physics RAS, 142432 Chernogolovka, Russia*

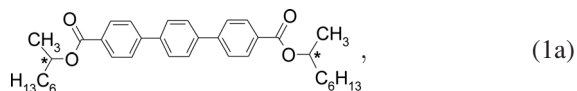
⁶*National Research Nuclear University «MEPhI», Kashirskoye shosse 31, 115409 Moscow, Russia*

(Received 27 October 2014; accepted 30 January 2015; published online 11 February 2015)

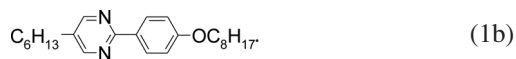
We report on a ferroelectric chiral smectic C (C*) phase obtained in a mixture of a nematic liquid crystal (NLC) and a chiral nonmesogenic dopant. The existence of C* phase was proven by calorimetric, dielectric and optical measurements, and also by X-rays analysis. The smectic C* which is obtained in such a way can flow, allowing to restore the ferroelectric liquid crystal layer structure in the electro-optical cells after action of the mechanical stress, as it happens with the cells filled with NLC. The proposed method of obtaining smectic C* material allows us to create innovative electro-optical cell combining the advantages of NLC (mechanical resilience) and smectic C* (high switching speed). © 2015 AIP Publishing LLC. [<http://dx.doi.org/10.1063/1.4908152>]

Smectic C* ferroelectric liquid crystals (FLC's) are of high demand due to their potential in fast display and photonic devices for different applications, operating in the microsecond range.^{1–3} The most appropriate and cheap method to design FLC composition with desirable properties is to admix a chiral dopant into a nonchiral smectic C matrix.⁴ The first step is to elaborate a smectic C matrix possessing the required properties, such as the necessary phase transitions sequence, low rotational viscosity, and appropriate molecular tilt angle. The second step is to select a chiral dopant providing acceptable values of spontaneous polarization and helix pitch.⁵

We have induced a chiral smectic C* phase by adding a nonmesogenic chiral dopant—the diester of optical active 2-heptanol and terphenyldicarboxylic acid (compound 1a),



to the nematic liquid crystal (NLC) 2-(4'-octyloxyphenyl)-5-hexyl-pyrimidine (compound 1b)



All binary mixtures, which have been used to construct the phase diagram at mixing of (1a) and (1b) compounds (Figure 1, transitions detected on heating), were investigated by differential scanning calorimetry, polarizing microscopy,

and dielectric and electro-optical methods.⁶ X-ray diffraction (XRD) analysis was performed as well.

The phase diagram shows that at the dopant concentration less than 4 mol % and temperature T above 28 °C, the only existing mesophase is the cholesteric (chiral nematic, N*) phase. At higher concentrations, the enantiotropic smectic C* and A* phases are induced.

At the dopant (1a) concentration of 19 mol %, the eutectic mixture (NFLC-1) occurs: there is no indication of two-phase regions, and the phase transitions sequence is: Cr → 12 °C → C* → 38 °C → A* → 59 °C → Is (where Cr stands for crystal phase and Is for isotropic phase, respectively). The

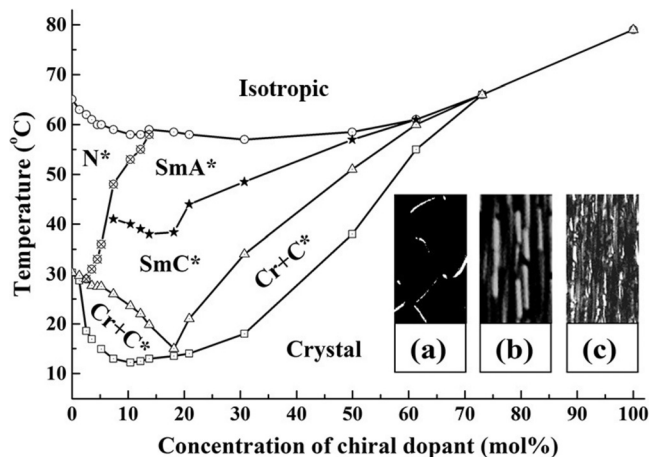


FIG. 1. Phase diagram of a binary mixture of NLC and non-mesogenic chiral dopant; “Cr + C*” indicates two phase regions, where both crystal and smectic C* phases coexist. The insets show liquid crystal textures (100 × 180 μm size) in the cells of thickness 1.7 μm placed between crossed polarizers: (a) cholesteric (N*) phase at 3 mol % of the chiral dopant, $T = 50$ °C; (b), (c) smectic A* phase, $T = 50$ °C, and smectic C* phase, $T = 30$ °C, at 19 mol % of the chiral dopant, respectively.

^{a)}Email: alfredo.strigazzi@polito.it

elaboration of such mixtures makes it necessary to prove their ferroelectric properties and to clarify its features in comparison with traditional FLC's. The most reliable method of identifying various liquid crystalline mesophases is XRD analysis. X-ray data were taken at the "Belok" beam line in the Kurchatov Synchrotron Centre (Moscow, Russia) using monochromatic radiation⁷ ($\lambda = 0.0984$ nm) at a sample-to-detector distance of 0.20 m. The LC material was placed in a circular opening (diameter about 0.5 mm) of a nylon loop. The two-dimensional (2D) X-ray scattering patterns were recorded with a Marresearch CCD detector (Rayonix SX165, 2048 \times 2048 pixels). Radial cross-sections of the 2D intensity distribution $I(q)$ were specified by averaging over narrow rectangular regions⁸ (q is the wave vector transfer). The measurements were performed for various compositions of the mixture presented at Figure 1 (in the range from 3 to 30 mol %), and in the whole temperature range up to isotropic phase.

Typically, we obtained powder-like 2D diffraction patterns, i.e., showing the uniform rings of scattering at different q values. In lamellar (smectic A* and smectic C*) phases, we observed two rings. The sharp ring in the small angle area corresponds to scattering from the stacks of smectic layers with periodicity of about 3 nm (depending on the composition of the mixture). The second broad ring is observed at larger angles (the corresponding distance is about 0.46 nm) and is due to short-range positional correlations between the molecules in the plane of layers.

In certain cases, the 2D diffraction patterns of well aligned smectic samples were registered, Figure 2(a). They clearly indicate that the broad diffuse crescents in the wide angle region are oriented nearly perpendicular to the

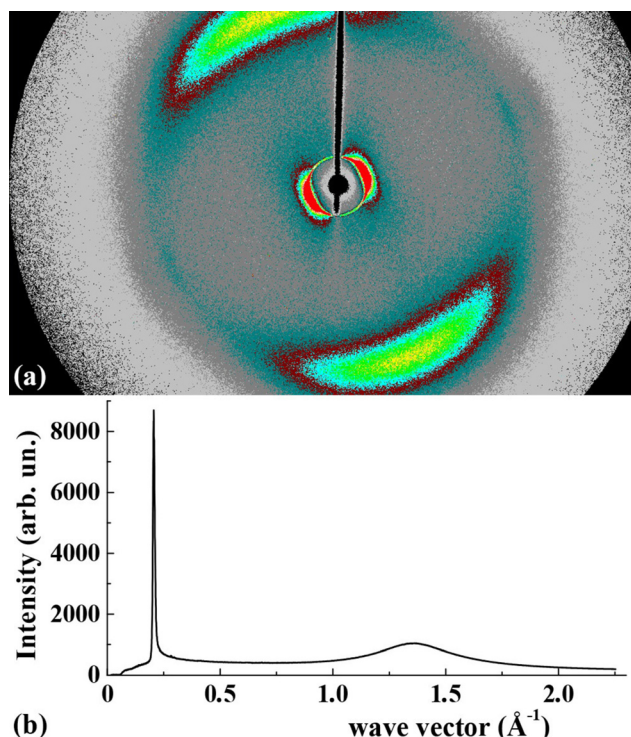


FIG. 2. (a) Two-dimensional X-ray scattering pattern in smectic C* phase of NFLC-1 at $T = 35$ °C; (b) the profile of diffraction pattern intensity.

direction of the layer normal, as it should be for the uniformly aligned smectic sample.⁹

The transition from smectic A* to smectic C* phase does not qualitatively change the above picture. However, the position of the sharp inner ring starts to shift in the direction of the larger angles, which corresponds to a decrease of the layer spacing due to the inclination of the molecules in the layers. Accordingly, the expression for the average tilt $\theta_{XR}(T)$ of the molecules in smectic layers, evaluated from XRD patterns, is given by

$$\theta_{XR}(T) = \arccos[d_C(T)/d_A(T_A)], \quad T_A > T_{C^*A^*}, \quad (1)$$

where d_C and d_A are the interlayer periodicities in the smectic C* and smectic A* phase, respectively, and T_A is a temperature in the A* phase. The formation of a Cr phase is signaled by the appearance of a large number of resolution limited peaks in the wide angle scattering area. The two phase regions (Cr + C*) are identified by the fact that the diffuse ring characteristic of the smectic phase coexists with the crystalline peaks.

Finally, we note that the existence of N* phase is proven by the significant broadening of the small angle lamellar peak at the transition to this phase. Figure 2(b) shows two peaks characterizing the C* phase: the sharp peak at small q gives the layer periodicity, while the broad peak gives the average distance between molecules in the plane of layers.

We evaluated the temperature dependencies of the tilt angle $\theta_{XR}(T)$ from XRD, using Eq. (1) (see Figure 3), and the spontaneous tilt angle $\theta_o(T)$ (i.e., the tilt angle in the absence of any electric field E) using the optical method.¹⁰ A direct measurement of θ_o is not possible for the mixtures consisting of (1a) and (1b) compounds by the reason of a significant contribution of the electroclinic effect¹¹ within the temperature range of both C* and A* phases. We emphasize that the direct measurements¹⁰ of the optical tilt angle requires application of an electric field $E > E_c$ (E_c is the critical field of the helix unwinding). The electric field induces some supplementary tilt $\theta_{ind}(T, E)$ owing to the electroclinic effect, in addition to spontaneous molecular tilt angle $\theta_o(T)$ in C* phase, and thereby, one can directly measure the angle θ_E , which is the sum of the angles $\theta_o(T)$ and $\theta_{ind}(T, E)$,

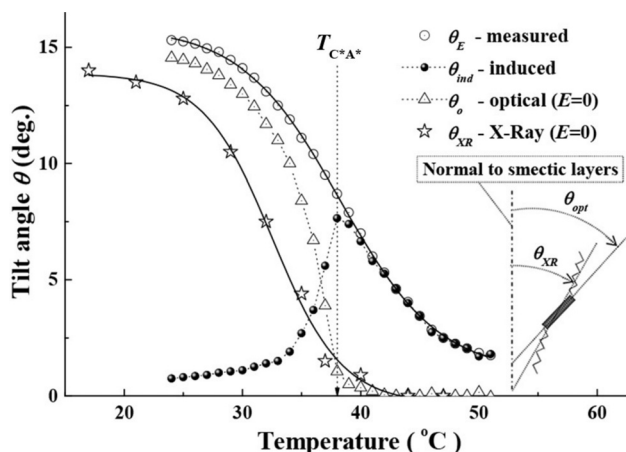


FIG. 3. Dependencies of NFLC-1 tilt angle on temperature. θ_E , θ_{ind} refer to the applied field $E_1 = 6.67$ V/ μ m. The inset shows the zig-zag model¹⁴ representation.

$$\theta_E(T, E) = \theta_0(T) + \theta_{ind}(T, E). \quad (2)$$

We have measured $\theta_E(T, E_i)$ at various T values for different fixed E_i values. The data for $\theta_E(T, E_1)$ at $E_1 = 6.67 \text{ V}/\mu\text{m}$ are shown in Figure 3. The spontaneous tilt $\theta_0(T)$ has been extracted as a zero term from the polynomial regression function, which fits the experimental $\theta_E(T, E)$ data at various $E > E_c$ for different fixed temperatures.¹² The $\theta_{ind}(T, E_1)$ dependence has been evaluated using Eq. (2).

The transition temperature $T_{C^*A^*}$ from C^* to A^* phase was evaluated due to analysis of the electroclinic effect.¹¹ The phase transition point corresponds to the maximum in temperature dependencies of the soft mode dielectric susceptibility¹³ or to the maximum of the electrically induced tilt angle θ_{ind} . The $\theta_{ind}(T, E_1)$ dependence (Figure 3) indicates $T_{C^*A^*} = 38^\circ\text{C}$.

The tilt angles measured by XRD are smaller than the angles measured by the electro-optical method (Figure 3). This result is in a good agreement with the zig-zag model.¹⁴ According to this model, the difference in tilt angles measured via XRD and by optical methods emerges due to the molecular alkyl tails flexibility, which is taken into account in the XRD method, whereas the optical method is sensitive to the inclination of the rigid central molecular core only. The application of the zig-zag model to NFLC-1 confirms that its layered structure is the same as in classical C and C^* phases.

The total polarization P_{tot} of a FLC cell, measured by means of the polarization reversal current integration method,¹⁵ is expressed as

$$P_{tot} = \chi_\infty E + P_E(T, E) = \chi_\infty E + P_s(T) + P_{ind}(T, E), \quad (3)$$

where χ_∞ is the component of the dielectric susceptibility responsible for the polarizability of the molecules which is present in all kind of dielectrics and $P_{ind}(T, E)$ is the polarization due to the electroclinic effect. The term $P_E(T, E)$ corresponds to polarization of FLC supramolecular structure

$$P_E(T, E) = \mu\theta_E(T, E), \quad (4)$$

where μ is the piezoelectric coupling coefficient. The experimental method we have used¹⁵ allows to measure directly

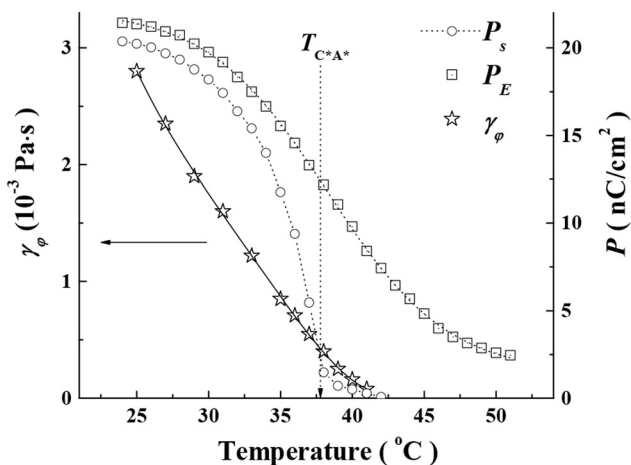


FIG. 4. Temperature dependencies of the spontaneous polarization P_s , and of the polarization P_E of the FLC supramolecular structure due to the electric field $E_1 = 6.67 \text{ V}/\mu\text{m}$ and rotational viscosity γ_ϕ of NFLC-1.

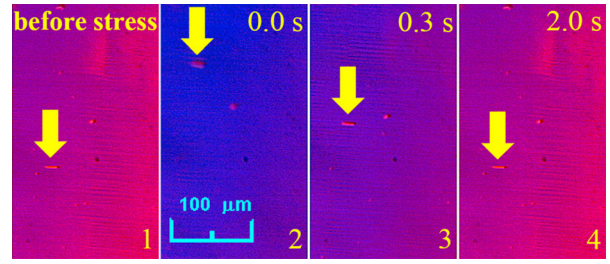


FIG. 5. Illustration of the relaxation flow in a cell filled with NFLC-1 after a mechanical stress. The arrow shows a direction parallel to smectic layers, indicates the position of the specially inserted marker, and forms 45° angle with the axis of the polarizer. Here, photo 1 corresponds to the initial state, before the stress application; it is identical to the final state (photo 4).

$P_E(T, E)$ (Figure 4) excluding $\chi_\infty E$ automatically. Referring to $\theta_E(T, E_1)$ (Figure 3) and Eq. (4), we have evaluated for NFLC-1 that $\mu \cong 80 \text{ nC}/\text{cm}^2\text{-rad}$, which is almost independent of E and T . Finally, the spontaneous polarization $P_s(T)$ has been extracted from experimental dependencies $\theta_E(T, E_1)$, $P_E(T, E_1)$, and $\theta_{ind}(T, E_1)$, with $E_1 = 6.67 \text{ V}/\mu\text{m}$, using Eqs. (2)–(4) (Figure 4).

Another method giving an estimate of the C^* to A^* phase transition temperature⁶ is based on the fact that the extremum of the pyroelectric coefficient $\gamma = dP_E/dT$ roughly coincides with $T_{C^*A^*}$. The coefficient γ was evaluated by differentiating the function $P_E(T, E_1)$ (Figure 3). The transition temperature $T_{C^*A^*} = 38.0^\circ\text{C} (\pm 0.2^\circ\text{C})$ was obtained by both methods.

Certainly, the soft mode plays a very prominent role in the electro-optical and dielectric behavior of NFLC-1 (and for all other mixtures with chiral dopant concentration greater than 4 mol % as well). In other words, we observe a very high sensitivity of smectic layers to the electric field.

We investigated the response of the NFLC-1 texture to a mechanical stress pulse (Figure 5). The photos of the textures illustrate the cell placed between crossed polarizers; the smectic layers are oriented perpendicular to the solid substrates. Photo 1 (Figure 5) represents a perfectly aligned $7 \mu\text{m}$ thick NFLC-1 cell before the application of the mechanical stress. Photo 2 depicts the same area in the cell just after the stress pulse, owing to which the cell thickness is reduced down to $4.7 \mu\text{m}$, as it follows from the analysis of birefringent colors.¹⁶

After the stress in the cell had been relieved, the relaxation process started (photo 3, Figure 5) with a motion of the material in the direction parallel to smectic layers planes. After 2 s, the cell came back to the initial state (photo 4). Any defect of the FLC monodomain alignment during the FLC flow within the cell was not detected.

The "shock-problem,"¹⁷ which means irreversible destruction of smectic layers structure under mechanical stress, does not manifest itself for this type of FLC, since NFLC-1 contains more than 80 mol % of the NLC (1b). The "shock-problem" occurs when the magnitude of deformation exceeds the elastic limit of the smectic layers deformation.¹⁸ This limit is extremely high for NFLC-1, since we were unable to detect it even when the FLC cell thickness was reduced by an order of magnitude under the mechanical pressure pulse. That is why strongly nonlinear elastic deformation

of the smectic layers could arise both in electric field and under the mechanical stress. This hypothesis could be supported by $\theta_{ind}(T, E_1)$ behavior (Figure 3), which does not obey Curie-Weiss law, as it is for nonlinear elastic deformation. In the case of linear elastic deformation of the smectic layers, the $P_s(T)$, $\theta_o(T)$, and $\theta_{XR}(T)$ dependencies should follow the classical square-root behavior in the mean-field approach, i.e., proportional to $(T_{C^*A^*} - T)^{1/2}$. On the contrary, in our experiments, a sigmoid shape flexure of the curves $P_s(T)$, $\theta_o(T)$, $\theta_{XR}(T)$ in the vicinity of $T_{C^*A^*}$ is observed (Figures 3 and 4).

Thus, the model of elasticity of the smectic layers is not applicable for the present very specific ferroelectric smectic C* phase. But, the identification of the origin of the "shock-free" smectic layers deformation goes far beyond the scope of this paper and will be the subject of further investigation.

Thereby, the elastic properties of NFLC-1 and the conventional FLC's are different, while their smectic layer structure is similar.¹⁴ This is also confirmed by the analysis of the rotational viscosity $\gamma_\phi(T)$ of NFLC-1 (Figure 4), which was measured by means of the electro-optical method.¹⁹

Using the obtained dependencies $\gamma_\phi(T)$ and $\theta_o(T)$ (Figure 3), we have found that $\gamma_\phi(\theta_o)$ is well described by the classical expression for the smectic C* phase ($\theta_o^2 \ll 1$)¹⁹

$$\gamma_\phi(T) = \alpha[\theta_o(T)]^2 \exp \beta[\theta_o(T)]^2, \quad (5)$$

where $\alpha = 0.034 \text{ Pa}\cdot\text{s}$ and $\beta = 9.7$ are constants depending only on the chemical structure of the molecules. Thus, one more evidence was obtained that we have to deal with the C* phase because Eq. (5) had been derived from the model of the entropy production in the typical smectic C* layers structure.¹⁹

Some considerable efforts have been applied to solve the "shock-problem." The first promising attempt goes back to 2006.²⁰ The most useful approaches were presented in the papers.^{18,21,22} The authors proposed the concept of long molecules of chiral tetra- or penta-phenyls in combination with short smectic C phenylpyrimidine molecules to create "shock-free" FLC's.

Our approach to solve the "shock-problem" greatly simplifies and reduces the cost of FLC fabrication because it allows using the commercially available NLC's. The electro-optical response time of the NFLC-1 ($30 \mu\text{s}$ at $T = 25^\circ\text{C}$ and $E = 3 \text{ V}/\mu\text{m}$) is an order of magnitude faster as compared to the former "shock-free" FLC's^{18,22} due to very low γ_ϕ value

(Figure 4). These properties of the "shock-free" FLC's offer good application prospects in advanced display and photonic devices.

This work was partially supported by RFBR project Nos. 13-02-00598, 13-02-90487 Ukr_f_a, and 15-59-32410. The participation of S. Sulyanov and B. Ostrovskii in this work was supported by Russian Science Foundation (Project No. 14-12-00475). The work at Kurchatov Synchrotron Centre was carried out in the framework of the Government Contract No. 14.619.21.0002. One of the authors (S. Torgova) acknowledges the support by Politecnico di Torino.

¹N. A. Clark and S. T. Lagerwall, *Appl. Phys. Lett.* **36**, 899 (1980).

²A. K. Srivastava, E. P. Pozhidaev, V. G. Chigrinov, and R. Manohar, *Appl. Phys. Lett.* **99**, 201106 (2011).

³E. P. Pozhidaev, A. K. Srivastava, A. D. Kiselev, V. G. Chigrinov, V. V. Vashchenko, A. I. Krivoshey, M. V. Minchenko, and H. S. Kwok, *Opt. Lett.* **39**, 2900 (2014).

⁴W. Kuczynski and H. Stegemeyer, *Chem. Phys. Lett.* **70**, 123 (1980).

⁵H. Stegemeyer, R. Meister, H.-J. Altenbach, and D. Szweczyk, *Liq. Cryst.* **14**, 1007 (1993).

⁶L. M. Blinov, M. I. Barnik, V. A. Baikov, L. A. Beresnev, E. P. Pozhidaev, and S. V. Yablonsky, *Liq. Cryst.* **2**, 121 (1987).

⁷D. M. Kheiker, M. V. Kovalchuk, Yu. N. Shilin, V. A. Shishkov, S. N. Sulyanov, P. V. Dorovatovskii, and A. A. Rusakov, *Cryst. Rep.* **52**, 358 (2007).

⁸S. N. Sulyanov, A. N. Popov, and D. M. Kheiker, *J. Appl. Cryst.* **27**, 934 (1994).

⁹B. I. Ostrovskii, *Structure and Bonding, Liquid Crystals I* (Springer, New York/Heidelberg, 1999), p. 199.

¹⁰B. I. Ostrovskii, A. Z. Rabinovich, A. S. Sonin, B. A. Strukov, and N. I. Chernova, *JETP Lett.* **25**, 70 (1977).

¹¹S. Garoff and R. B. Meyer, *Phys. Rev. Lett.* **38**, 848 (1977).

¹²K. Saxena, L. Beresnev, L. Blinov, S. Pikin, and W. Haase, *Ferroelectrics* **213**, 73 (1998).

¹³E. P. Pozhidaev, L. M. Blinov, L. A. Beresnev, and V. V. Belyaev, *Mol. Cryst. Liq. Cryst.* **124**, 359 (1985).

¹⁴R. Bartolino, J. Doucet, and G. Durand, *Ann. Phys.* **3**, 389 (1978).

¹⁵V. Panov, J. K. Vij, and N. M. Shtykov, *Liquid Crystals* **28**, 615 (2001).

¹⁶G. Hegde, P. Xu, E. Pozhidaev, V. Chigrinov, and H. S. Kwok, *Liq. Cryst.* **35**, 1137 (2008).

¹⁷N. Wakita, T. Uemoda, and H. Ohnishi, *Ferroelectrics* **149**, 229 (1993).

¹⁸V. Lapanik, V. Bezborodov, S. Timofeev, and W. Haase, *Appl. Phys. Lett.* **97**, 251913 (2010).

¹⁹E. P. Pozhidaev, M. A. Osipov, V. G. Chigrinov, V. A. Baikov, L. M. Blinov, and L. A. Beresnev, *J. Exp. Theor. Phys.* **67**(2), 283 (1988).

²⁰V. Bezborodov, V. Lapanik, G. Sasnouski, and W. Haase, *Ferroelectrics* **343**, 49 (2006).

²¹V. S. Bezborodov, V. I. Lapanik, G. M. Sasnouski, and W. Haase, *Liq. Cryst.* **40**, 1383 (2013).

²²V. Lapanik, V. Bezborodov, G. Sasnouski, and W. Haase, *Liq. Cryst.* **40**, 1391 (2013).